

# Boron Complexes of Tridentate Acyl Pyridylhydrazones

Alexander E. R. Watson,<sup>[a]</sup> Paul D. Boyle,<sup>[a]</sup> Paul J. Ragogna,<sup>\*[a]</sup> and Joe B. Gilroy<sup>\*[a]</sup>

Since the development of the chemistry and applications of boron dipyrromethene dyes (BODIPYs), numerous other platforms based on boron complexes of *N*-donor ligands have emerged as molecular optoelectronic materials. By tailoring the structure of the ligand bound to boron, the optical and electronic properties of a compound can be precisely tuned for unique properties, such as aggregation-induced emission (AIE) in the case of boron difluoride hydrazones (BODIHs). We examine the impact of modifying the typical bidentate hydrazone ligand structure used to prepare BODIHs to enable

a tridentate coordination mode to produce boron complexes of tridentate acyl pyridylhydrazones. This change allows for the use of arylboronic acids as sources of boron and facilitates the inclusion of complex organic components at the boron centre, including the formation of dye-dye conjugates. The synthesized compounds exhibit distinct optical and electronic properties when compared to BODIHs, such as reversible electrochemical reduction and up to a >300 nm *pseudo*-Stokes shift in the solid state, all of which were supported by density functional theory calculations.

## Introduction

The development of new  $\pi$ -conjugated materials is vital to addressing their myriad of applications. From sensing<sup>[1]</sup> to bioimaging<sup>[2]</sup> or use in photovoltaics<sup>[3]</sup> and organic light-emitting diodes (OLEDs),<sup>[4]</sup> each application demands a different set of properties from a given material. Following the extensive application of boron dipyrromethene dyes (BODIPY, I)<sup>[5,6]</sup> the incorporation of boron into conjugated *N*-donor ligands has emerged as a common strategy in the design of molecular optoelectronic materials.<sup>[7–9]</sup>

By changing the structure of ligands, the photophysical properties of the resultant complexes with boron can be finely manipulated. For example, appending large  $\pi$ -conjugated substituents to a ligand is a common strategy to access near-IR photoluminescence.<sup>[10]</sup> Another common strategy is to employ electron donating and withdrawing groups in tandem to create “push-pull” fluorophores with large Stokes shifts.<sup>[11]</sup> The inclusion of large, freely rotating substituents often induces a phenomenon known as aggregation-induced emission (AIE), where a compound is emissive in the aggregate or solid state due to the restriction of intramolecular rotation (RIM).<sup>[12]</sup> This is the principle on which boron difluoride hydrazones (BODIHs, II) distinguish themselves from most conventional organic fluorophores, which often see their emission quenched in the

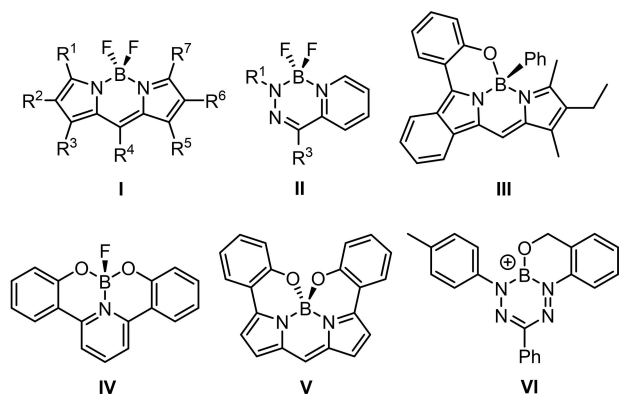
solid state. BODIH chemistry was pioneered by the Aprahamian group<sup>[13–19]</sup> and has also been studied by the Gilroy group and others.<sup>[20–28]</sup> In search of novel structures and properties, further iterations of BODIH syntheses have involved modifications to the peripheral structure.<sup>[16]</sup> This includes variants functionalized with electron-withdrawing and donating groups,<sup>[13]</sup> dimerization through different sites on the ligand,<sup>[22–24]</sup> and the incorporation of a benzothiazole group in place of pyridine.<sup>[25,26,29]</sup> BODIHs have also been incorporated into polymers, resulting in unique AIE and viscosity sensing compared to their molecular analogues.<sup>[21]</sup> All of these derivatives focus on bidentate ligands. The effect of increasing the denticity of the ligand has not been explored.

Increasing ligand denticity has been reported to have a variety of effects on the properties and structure of the resultant boron adducts.<sup>[30]</sup> Chen and coworkers designed a tridentate dipyrromethene ligand that extended  $\pi$ -conjugation and resulted in a boron complex (III) with near-infrared emission.<sup>[31]</sup> A tridentate hydroxyphenylpyridine compound (IV) exhibits white electroluminescence, with modified variants being used in TADF-based organic light-emitting diodes (OLEDs).<sup>[32,33]</sup> Tridentate or tetradentate ligands are also capable of introducing chirality to the molecule, enabling circularly-polarized luminescence (CPL), such as the helically chiral boron complex of a tetradentate dipyrin ligand (V) designed by Alnoman and co-workers, based on earlier work by Burgess *et al.*<sup>[34,35]</sup> Increasing ligand denticity has also been demonstrated to enable the facile support of low valent or reactive main group species, such as a borenium cation supported by a tridentate formazanate (VI).<sup>[36]</sup>

[a] A. E. R. Watson, Dr. P. D. Boyle, Prof. Dr. P. J. Ragogna, Prof. Dr. J. B. Gilroy  
Department of Chemistry  
The University of Western Ontario (Western University)  
1151 Richmond Street North, Ontario, N6A 5B7, London  
E-mail: pragogna@uwo.ca  
joe.gilroy@uwo.ca

Supporting information for this article is available on the WWW under <https://doi.org/10.1002/ejoc.202400132>

© 2024 The Authors. European Journal of Organic Chemistry published by Wiley-VCH GmbH. This is an open access article under the terms of the Creative Commons Attribution Non-Commercial NoDerivs License, which permits use and distribution in any medium, provided the original work is properly cited, the use is non-commercial and no modifications or adaptations are made.



Acyl hydrazones are easily prepared through the condensation of a hydrazide and a ketone or aldehyde. This robust linkage has featured in molecular photoswitches and rotaxanes,<sup>[37,38]</sup> as well as in several related boron adducts.<sup>[39–42]</sup> This work involves the synthesis of boron complexes of acyl pyridylhydrazones and an examination of their optical and electronic properties. The synthesis of these compounds represents an accessible route to increase the denticity of a typical hydrazone ligand and subsequently realize new optical and electronic properties.

## Results and Discussion

The preparation of ligands **1a** and **1b** involved the condensation of salicylhydrazide with the requisite 2-pyridylketone (Scheme 1). The presence of two downfield, broad singlets in the <sup>1</sup>H NMR spectra (**1a**: 15.57, 12.34 ppm; **1b**: 11.80, 11.47 ppm) confirmed the successful synthesis of these ligands (Figure S1–S4). Similar tridentate pyridylhydrazone ligands are known in transition metal chemistry, though they typically coordinate to transition metals in an N,O,O' fashion through the azine tautomer of the ligand.<sup>[43–46]</sup>

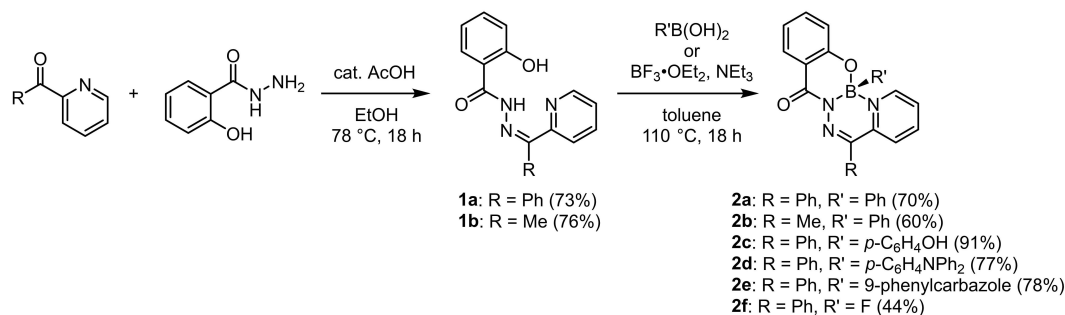
The incorporation of boron to afford compounds **2a–e** was achieved by heating the hydrazone ligand with an arylboronic acid (Scheme 1). These syntheses did not require an inert atmosphere or the use of any oxygen and moisture-sensitive reagents, such as the haloboranes typical to the synthesis of many similar boron adducts. The preparation of compounds

**Table 1.** Select metrics of the solid-state structures of compounds **2a**, **2d**, and **2f**.

Compound	Salicyloyl-pyridine angle (°)	B(1)–O(2) bond length (Å)	B(1)–N(1) bond length (Å)	B(1)–N(3) bond length (Å)
<b>2a</b>	7.93(5)	0.4692(12)	1.4600(11)	1.5851(12)
<b>2d</b>	14.73(7)	0.5609(14)	1.4577(13)	1.5865(14)
<b>2f</b>	30.30(6)	0.6161(16)	1.4345(15)	1.5767(17)

**2c–e** also tolerated substitution of the arylboronic acid to include a hydroxyl group, diphenylamine, and carbazole at the *para* position. Upon boron coordination, the downfield <sup>1</sup>H NMR resonances corresponding to the OH and NH groups were no longer observed, and a singlet at approximately 3 ppm appears in the <sup>11</sup>B NMR spectra (Figures S5–S19). Both observations were consistent with the incorporation of a tetracoordinate boron centre. Compound **2f** had a more elaborate preparation, which involved heating with excess BF<sub>3</sub>·OEt<sub>2</sub> and NEt<sub>3</sub> under an inert atmosphere. The lone B–F bond in compound **2f** was associated with a characteristic doublet in the <sup>11</sup>B NMR spectrum (0.6 ppm, <sup>1</sup>J<sub>BF</sub> = 42.1 Hz) and quartet in the <sup>19</sup>F NMR spectrum (–139.8 ppm, <sup>1</sup>J<sub>BF</sub> = 43.5 Hz) (Figures S20–S23). All of compounds **2a–f** were produced as racemates, as they were found to be optically inactive.

Single crystals of compounds **2a**, **2d**, and **2f** were grown and analyzed via X-ray diffraction (Figure 1, Table S1).<sup>[47]</sup> The solid-state structures of all three compounds featured a tetracoordinate boron atom chelated in an N,N',O fashion to the hydrazone tautomer of the ligand. Electronic delocalization was evident throughout the hydrazone backbone by the bond lengths having intermediate values between their respective single and double bonds. The planarity of the complexes, as quantified by the angle between the pyridyl and salicyloyl aryl rings, varied depending on the boron substituent (Table 1). Compound **2a** was the most planar, with a smaller angle (7.93(5)°) between the planes defined by the salicyloyl and pyridyl rings than **2d** (14.73(7)°), and **2f** was the least planar (30.30(6)°). Increased planarity coincided with a smaller displacement of the boron atom from the plane of the pyridylhydrazone ligand (N(1)–N(2)–C(1)–C(2)–N(3)). The more planar **2a** had the smallest boron displacement (0.4692(12) Å),



**Scheme 1.** Synthesis of ligands **1a** and **1b**, and boron complexes **2a–f**.

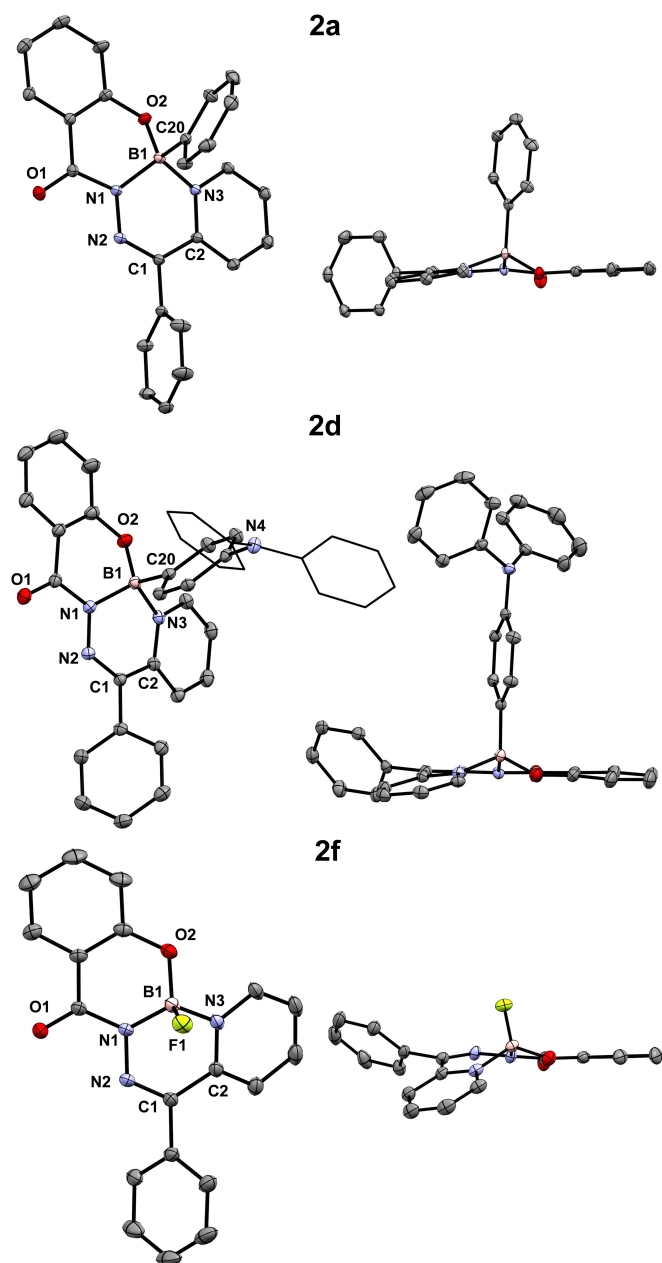


**Figure 1.** Top (left) and side (right) views of the solid-state structures of boron complexes **2a**, **2d**, and **2f**. Hydrogen atoms are omitted for clarity. Select phenyl substituents are shown in wireframe for clarity. Anisotropic displacement ellipsoids are displayed at a 50% probability level.

followed by **2d** (0.5609(14) Å) and then **2f** (0.6161(16) Å). The bond lengths at boron differed between all three solid-state structures. The compounds containing boron bound to an aryl ring had shorter bonds to their anionic oxygen and nitrogen donor atoms (**2a**: B(1)–O(2) 1.4600(11) Å, B(1)–N(1) 1.5440(12) Å; **2d**: B(1)–O(2) 1.4577(13) Å, B(1)–N(1) 1.5417(13) Å) than the boron centre bound to the electron-withdrawing fluorine substituent (**2f**: B(1)–O(2) 1.4345(15) Å, B(1)–N(1) 1.5207(16) Å). The solid-state packing of compound **2d** exhibited several close intermolecular interactions, such as C–H... $\pi$  interactions ranging from 2.780 to 2.872 Å and a close C–H...O interaction of 2.701 Å (Figure S24).

To rationalize the experimental findings concerning the electronic structure of these compounds, density functional theory (DFT) calculations were performed using the LC- $\omega$ hPBE functional ( $\omega = 0.14$ ), DGDZVP2 basis set, and CPCM method of implicit solvation ( $\text{CH}_2\text{Cl}_2$ ).<sup>[48,49]</sup> The predicted  $\lambda_{\text{max}}$  values for boron complexes **2a–f** were over-estimated by approximately 40 nm, but closely followed the trend of the experimental values (Table 2 and Table S2). These lowest energy transitions were generally associated with HOMO→LUMO transitions with compound **2e** being the exception. In this case, the lowest energy excitation was dominated by the HOMO–1 and LUMO orbitals.

Molecular orbitals of **2a–f** were modelled (Figure 2) and showed that the HOMOs of **2a–2c** and **2f** are delocalized across the entire molecule in a manner typical of BODIHYs.<sup>[20]</sup> Dye-dye conjugates **2d** and **2e** exhibited HOMOs entirely localized to the triphenylamine or 9-phenylcarbazole substituents, and LUMOs localized to the boron hydrazone component. This suggested that these compounds may exhibit intramolecular charge transfer and rationalized the single low energy maxima observed in the solid and aggregate-state photoluminescence data (*vide infra*). While the LUMO energies were all within a small range (–1.69 to –1.83 eV), the HOMO energies varied to a greater extent. Compounds **2d** and **2e** had the highest energy HOMOs at –6.39 and –6.84 eV, respectively, and compound **2f** the lowest energy HOMO at –7.56 eV. The LUMOs of the same compounds were primarily localized to the annulated  $\text{C}_2\text{N}_3\text{B}$  and pyridine ring system, along with some electron density on the C=O bond.

The electronic properties of compounds **2a–f** were analyzed using UV-vis absorption and photoluminescence spectroscopy in both  $\text{CH}_2\text{Cl}_2$  solution and as thin films (Table 2, Figures 3a and 3b). The  $\lambda_{\text{max}}$  of compounds **2a–c** remained similar at approximately 398 to 414 nm in both the solution and solid states. Dye-dye conjugates **2d** and **2e** exhibited a separate absorption feature corresponding to the triphenylamine and carbazole functional groups, respectively (**2d**:  $\lambda_{\text{max}} = 302$  nm; **2e**:  $\lambda_{\text{max}} = 293$ ). Compound **2f** had a hypsochromically shifted  $\lambda_{\text{max}}$  of 380 nm compared to compounds **2a–e**, given the electron-withdrawing fluorine substituent at boron.

The photoluminescence exhibited by this series of compounds in  $\text{CH}_2\text{Cl}_2$  solution is weak, with  $\Phi_{\text{PL}}$  values no greater than 0.01. Compounds **2a–c** all displayed  $\lambda_{\text{PL}}$  at 495 nm. Compound **2f** had a hypsochromically shifted  $\lambda_{\text{PL}}$  at 454 nm in solution, in accordance with its lower  $\lambda_{\text{max}}$  than **2a–e**. Also of note was the dual state emission featured in the dye-dye conjugates **2d** and **2e**, where in addition to the typical emission peak at ~500 nm there were discrete emission maxima associated with the triphenylamine or phenylcarbazole moiety, respectively (**2d**: 401 nm; **2e**: 345 and 360 nm).<sup>[50,51]</sup> BODIHYs usually exhibit weak photoluminescence in solution due to non-radiative decay resulting from the presence of appended aryl rotors. It was thought that by eliminating some or all of the ligand-appended aryl rotors (*i.e.*, **2b**) efficient solution emission could be realized, but this was not the case.

Compounds **2a–f** exhibited higher  $\Phi_{\text{PL}}$  as thin films, and the  $\lambda_{\text{PL}}$  remained similar. The exception to this trend was the

Compound	State	$\lambda_{\text{max}}$ (nm)	$\epsilon$ ( $\text{M}^{-1} \text{cm}^{-1}$ )	$\lambda_{\text{PL}}$ (nm)	$\Phi_{\text{PL}}$ (%)
2a	CH <sub>2</sub> Cl <sub>2</sub>	414	9200	495	< 1
	thin film	413	–	498	1
2b	CH <sub>2</sub> Cl <sub>2</sub>	403	8300	495	< 1
	thin film	398	–	492	3
2c <sup>[a]</sup>	CH <sub>2</sub> Cl <sub>2</sub>	414	9500	495	< 1
2d	CH <sub>2</sub> Cl <sub>2</sub>	302	31000	401, 507	–
		414	9500	507	< 1
	thin film	303	–	415, 607	–
		415	–	607	1
2e	CH <sub>2</sub> Cl <sub>2</sub>	293	30800	360, 505	–
		412	9500	606	< 1
	thin film	295	–	549	–
		414	–	541	2
2f	CH <sub>2</sub> Cl <sub>2</sub>	380	13100	454	1
	thin film	378	–	448	2

[a] Due to the limited solubility of 2c, thin films of an appropriate quality could not be made.

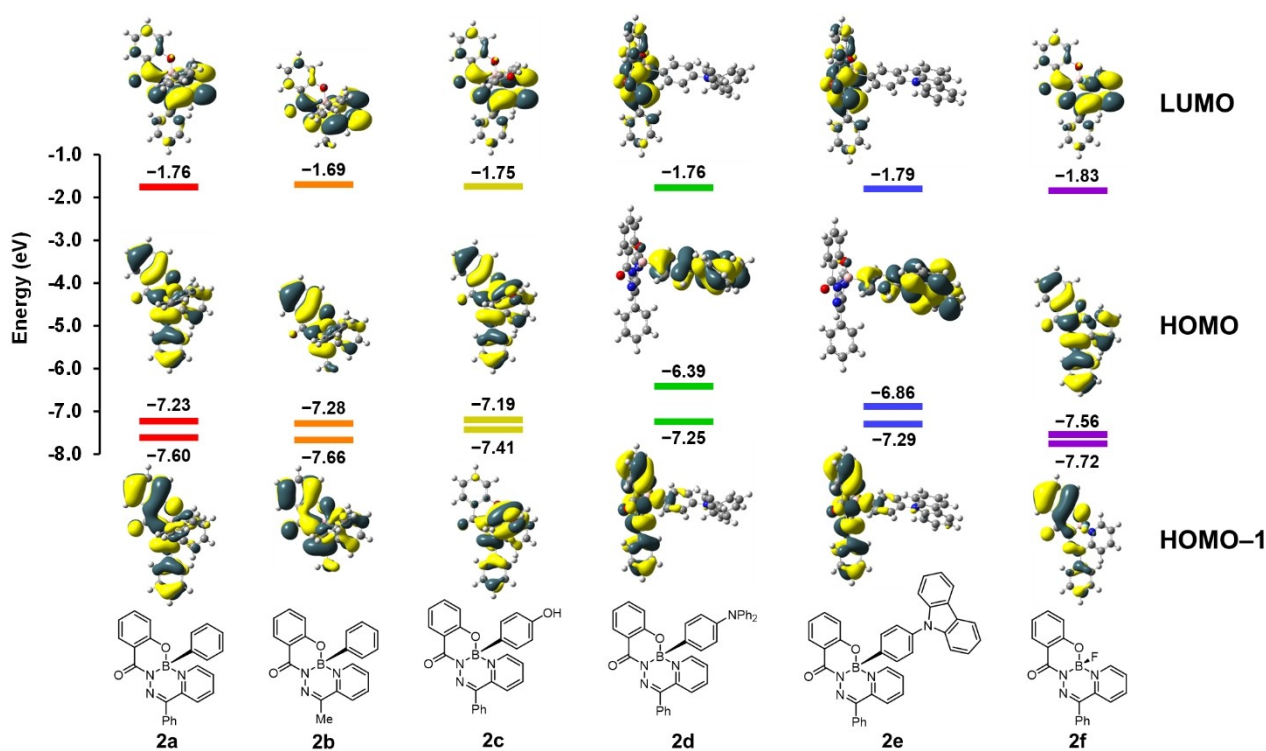
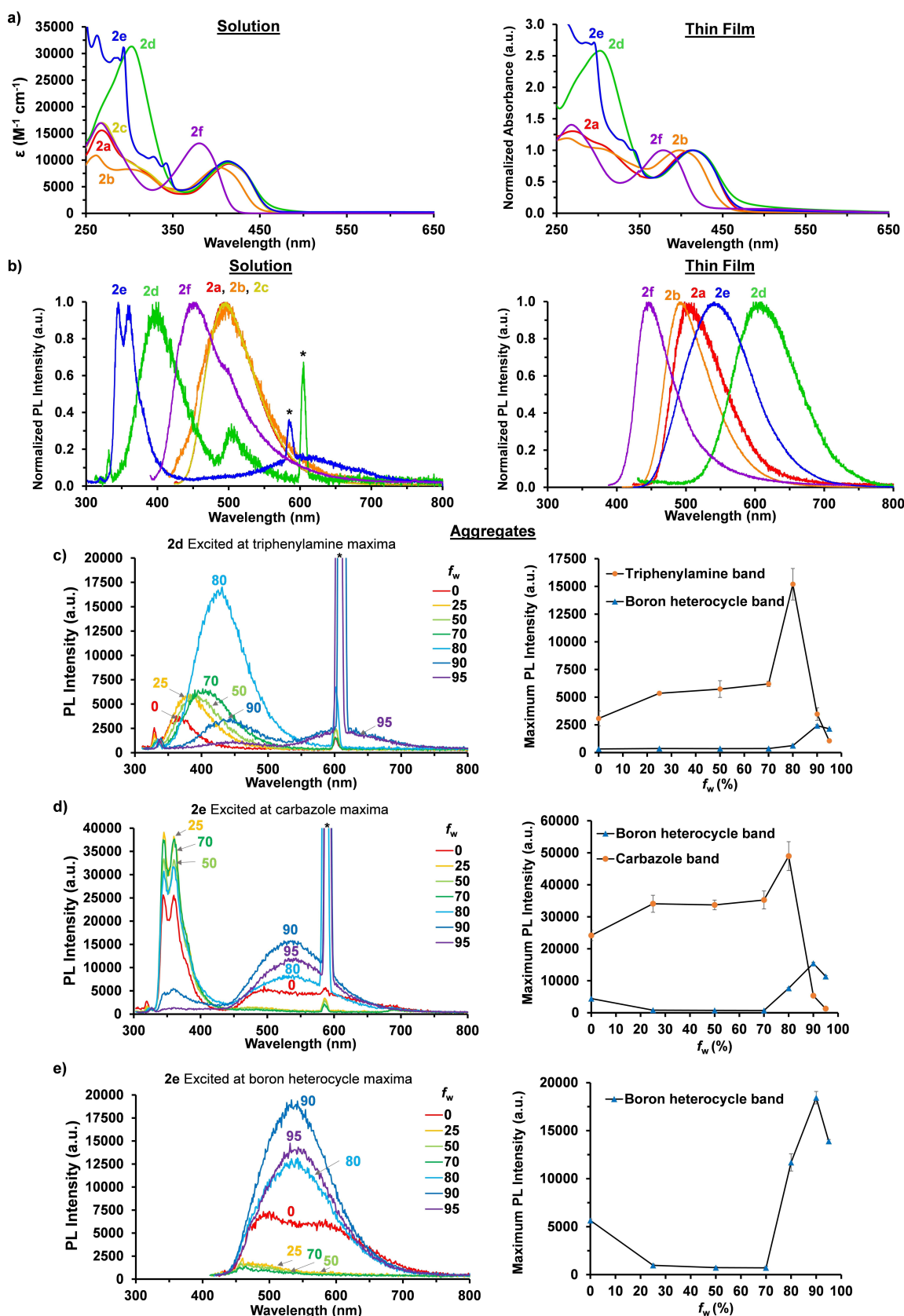


Figure 2. Computed molecular orbitals of 2a–f (ground state, LC- $\omega$ hPBE ( $\omega = 0.14$ )/DGDZVP2 SCRf = (CPCM, solvent = CH<sub>2</sub>Cl<sub>2</sub>) method).

changes in  $\lambda_{\text{PL}}$  for the triphenylamine-containing dye 2d. Instead of two independent maxima, as was observed in solution, there was a single bathochromically shifted  $\lambda_{\text{PL}}$  at 607 nm, yielding a large *pseudo*-Stokes shift of 16 500  $\text{cm}^{-1}$  (304 nm). Compound 2e exhibited a similar phenomenon with a  $\lambda_{\text{PL}}$  at 549 nm, resulting in a *pseudo*-Stokes shift of 15 700  $\text{cm}^{-1}$  (254 nm).

Dye-dye conjugates 2d and 2e possessed significant bathochromic shifts in their photoluminescence spectra, especially in the solid state, when compared to compounds 2a–2c and

2f. In the DFT calculations, the localization of the LUMO to the triphenylamine or phenylcarbazole donor and the HOMO to the boron heterocycle core (Figure 2) suggested a degree of intramolecular charge transfer may have been operative for these compounds, which is known to result in bathochromically-shifted  $\lambda_{\text{PL}}$ .<sup>[52]</sup> The solid-state packing of 2d exhibited C–H $\cdots$  $\pi$  and C–H $\cdots$ O interactions ranging from 2.701 to 2.806 Å (Figure S24). Short intermolecular interactions such as these are known to lead to intermolecular charge transfer and bathochromically-shifted  $\lambda_{\text{PL}}$ .<sup>[53,54]</sup>



**Figure 3.** a) UV-vis absorption spectra of 2a–f as 15  $\mu M$   $CH_2Cl_2$  solutions (left) and 2a, 2b, and 2d–f as thin films on a quartz glass substrate (right). b) UV-vis photoluminescence spectra of 2a–f as 15  $\mu M$   $CH_2Cl_2$  solutions (left) and 2a, 2b, and 2d–f as thin films on a quartz glass substrate (right). Second-order scattering peaks are denoted by \*. Due to the limited solubility of an appropriate quality could not be made. c–e) UV-vis photoluminescence spectra of THF-water mixtures of c) compound 2d excited at the triphenylamine-based  $\lambda_{max}$ , d) compound 2e excited at the carbazole-based  $\lambda_{max}$ , and e) compound 2e excited at the boron heterocycle-based  $\lambda_{max}$ , all alongside a plot of maximum photoluminescence intensity at different water fractions ( $f_w$ ).

As BODIHYs are well-known for their AIE, dilute solutions of compounds **2a–f** in THF were made, and varying amounts of water were added to induce aggregation. When analyzed via UV-vis absorption and emission spectroscopy, it was observed that as the amount of water in the mixture increased, emission intensity decreased for **2a–c** and **2f** (Figure S25–S28). This was consistent with an aggregation-caused quenching mechanism experienced by many organic fluorophores.<sup>[55]</sup>

Dye-dye conjugates **2d** and **2e** experienced aggregation-induced emission enhancement (AIEE) to differing extents depending on which local maxima was excited (Figures 3c–e, S29 and S30, Table 3). In triphenylamine-appended **2d** there was an absorption maximum at approximately 300 nm, associated with the triphenylamine moiety, and a second lower energy maxima at ~410 nm associated with the boron heterocycle core. Excitation at the high energy absorption maxima (associated with the triphenylamine moiety) resulted in two photoluminescence peaks at 426 and 609 nm, and maximum photoluminescence intensities were observed at water volume fractions ( $f_w$ ) of 80 and 90%. This represented enhancement factors of 4.9 and 7.4, respectively, when compared to the photoluminescence intensities of the pure THF solutions. Exciting at the lower energy boron heterocycle-based absorption maxima (~410 nm) did not result in appreciable photoluminescence. The AIEE behaviour of carbazole-appended **2e** was also dependent on whether the molecule was excited at the carbazole-based maxima (~293 nm) or boron heterocycle-based maxima (~410 nm). Exciting at the higher energy maxima resulted in two photoluminescence maxima at 359 and 538 nm which exhibited their highest emission intensities at 80 and 90%  $f_w$ , respectively. Smaller enhancement factors of 2 to 3 were observed because of its significant photoluminescence in solution. The observation of low energy photoluminescence peaks at 609 nm (**2d**) and 538 nm (**2e**) were consistent with the thin film photoluminescence data.

The redox behaviour of boron complexes **2a–2f** were probed using cyclic voltammetry (Figure 4, Table 4). Compounds **2a–2d** exhibited reversible reduction waves at similar voltages ranging from –1.60 to –1.73 V. These similar reduction potentials were rationalized by the similar LUMO energies computed in the DFT calculations. Compounds **2e** and **2f** featured irreversible reduction events in a similar range. Only compounds **2d** and **2e** exhibited oxidation events within the solvent stability window, which were associated with the appended redox-active diphenylamine (**2d**) and carbazole (**2e**)

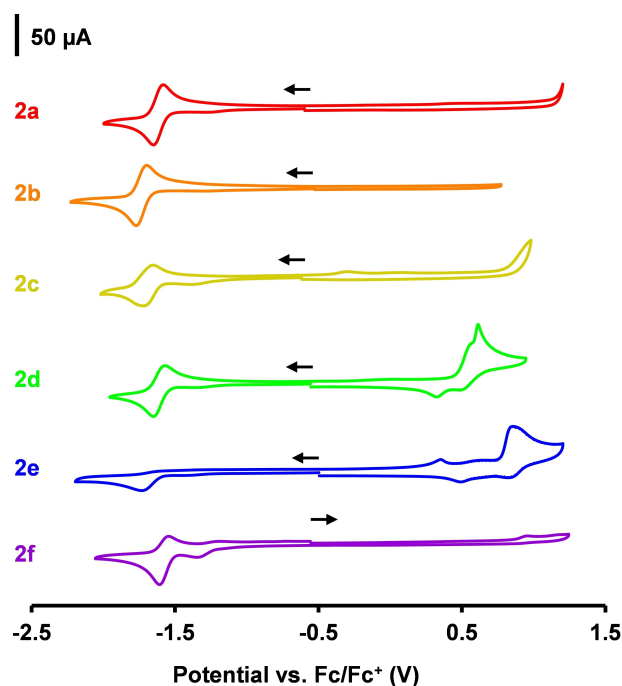


**Figure 4.** Cyclic voltammograms recorded for 0.1 mM solutions of **2a–f** in dry, degassed  $\text{CH}_3\text{CN}$  with 0.1 M  $[\text{nBu}_4\text{N}][\text{PF}_6]$  as supporting electrolyte. The scan rate was  $250 \text{ mV s}^{-1}$  and the arrows denote initial scan directions.

Table 4. Reduction and oxidation potentials of compounds <b>2a–f</b> . <sup>[a]</sup>		
Compound	$E_{\text{red}}$ (V)	$E_{\text{ox}}$ (V)
<b>2a</b>	–1.62	–
<b>2b</b>	–1.73	–
<b>2c</b>	–1.69	–
<b>2d</b>	–1.60	0.62 <sup>[b]</sup>
<b>2e</b>	–1.71 <sup>[b]</sup>	0.87 <sup>[b]</sup>
<b>2f</b>	–1.57 <sup>[b]</sup>	–

[a] Cyclic voltammetry experiments were performed at scan rates of  $250 \text{ mV s}^{-1}$  in dry, degassed solutions of  $\text{CH}_3\text{CN}$ , containing ~1 mM analyte, and 0.1 M  $[\text{nBu}_4\text{N}][\text{PF}_6]$  as the supporting electrolyte and were internally referenced against the ferrocene/ferrocenium redox couple. [b] Redox event was irreversible, and the potential at maximum anodic or cathodic current is reported.

moieties.<sup>[56,57]</sup> This electrochemical redox behaviour differed substantially from the redox behaviour of bidentate BODIHYs,

Table 3. UV-vis emission spectroscopy of THF/water mixtures of <b>2d</b> and <b>2e</b> with the greatest photoluminescence intensities.					
Compound	Component excited	$\lambda_{\text{ex}}$ (nm) <sup>[a]</sup>	$\lambda_{\text{PL}}$ (nm)	$f_w$ (%)	Enhancement factor
<b>2d</b>	triphenylamine	301	426	80	4.9
	triphenylamine	305	609	90	7.4
	boron heterocycle <sup>[b]</sup>	–	–	–	–
<b>2e</b>	carbazole	293	359	80	2.0
	carbazole	294	538	90	3.5
	boron heterocycle	409	540	90	3.3

[a] Mixtures were excited at the highest energy  $\lambda_{\text{max}}$  associated with each component. [b] No appreciable photoluminescence was observed.

which featured irreversible reductions at approximately  $-1.80$  V and oxidations ranging from  $0.62$  to  $1.02$  V.<sup>[20]</sup> This demonstrated that increased denticity was a compelling tool for tuning the electronic structure of  $\pi$ -conjugated molecules.

## Conclusions

Boron complexes of tridentate acyl pyridylhydrazones, a new platform of boron-containing  $\pi$ -conjugated materials, were investigated. These compounds were easily prepared through condensation with arylboronic acids or treatment with  $\text{BF}_3 \cdot \text{OEt}_2$ , with the former enabling facile functionalization at boron. Compared to BODIHYs, the ability to incorporate boron using arylboronic acids enabled a host of unique architectures that are not possible with  $\text{BF}_2$ -containing dyes. Instead, boron became a point of further functionalization, such as the donor-acceptor architecture exhibited by dye-dye conjugates **2d** and **2e**. When comparing the optoelectronic properties of compound **2f** to an archetypical BODIHY (II,  $\text{R}^1=\text{R}^3=\text{Ph}$ ), the differences of using a tridentate ligand become evident. In  $\text{CH}_2\text{Cl}_2$  solution both the  $\lambda_{\text{max}}$  and  $\lambda_{\text{em}}$  of compound **2f** ( $\lambda_{\text{max}}=380$  nm,  $\lambda_{\text{em}}=454$  nm) were hypsochromically shifted relative to BODIHY (II,  $\text{R}^1=\text{R}^3=\text{Ph}$ ;  $\lambda_{\text{max}}=437$  nm,  $\lambda_{\text{em}}=540$  nm), and the same trend was followed in the solid state.<sup>[15]</sup> Compound **2f** was emissive in solution, in the solid-state and aggregate-state, while BODIHY (II,  $\text{R}^1=\text{R}^3=\text{Ph}$ ) was only emissive in the solid or aggregate-states. BODIHYs are natively AIE-active, while the tridentate variants require specific functionalization (*i.e.*, **2d**, **2e**). The majority of the synthesized compounds in this study exhibited reversible reductions, while BODIHYs only exhibited reversible oxidations when the *para* position of their  $\text{R}^1$  phenyl substituent was blocked. Further exploration of these tridentate boron complexes as new heterocyclic motifs will work toward tuning their emission maxima and quantum yields. These conclusions will be used to inform further iterations of this ligand system by leveraging the synthetic diversity afforded by using arylboronic acids.

## Supporting Information

The authors have cited additional references within the Supporting Information.<sup>[48,49,58–64]</sup>

## Acknowledgements

The authors thank the University of Western Ontario, the Natural Science and Engineering Research Council (NSERC) of Canada (PGS–D scholarship to A.E.R.W.; Grant DG RGPIN-2021-04377 to P.J.R.; Grant DG, RGPIN-2018-04240 to J.B.G.), the Ontario Ministry of Research and Innovation (Grant ER14-10-147 to J.B.G.), the Canada Foundation for Innovation (Grant JELF 33977 to J.B.G.), the Digital Research Alliance of Canada, and Solvay for supporting this work.

## Conflict of Interests

The authors declare no conflict of interest.

## Data Availability Statement

The data that support the findings of this study are available in the supplementary material of this article.

**Keywords:** boron · cyclic voltammetry · fluorescence · hydrazones · UV-vis spectroscopy

- [1] S. Rochat, T. M. Swager, *ACS Appl. Mater. Interfaces* **2013**, *5*, 4488–4502.
- [2] K.-Y. Pu, B. Liu, *Adv. Funct. Mater.* **2011**, *21*, 3408–3423.
- [3] Y. Lin, Y. Li, X. Zhan, *Chem. Soc. Rev.* **2012**, *41*, 4245–4272.
- [4] Q. Wei, N. Fei, A. Islam, T. Lei, L. Hong, R. Peng, X. Fan, L. Chen, P. Gao, Z. Ge, *Adv. Opt. Mater.* **2018**, *6*, 1800512.
- [5] A. Loudet, K. Burgess, *Chem. Rev.* **2007**, *107*, 4891–4932.
- [6] M. Poddar, R. Misra, *Coord. Chem. Rev.* **2020**, *421*, 213462.
- [7] D. Frath, J. Massue, G. Ulrich, R. Ziessel, *Angew. Chem. Int. Ed.* **2014**, *53*, 2290–2310.
- [8] M. J. D. Bosdet, W. E. Piers, *Can. J. Chem.* **2009**, *87*, 8–29.
- [9] S. K. Mellerup, S. Wang, *Trends Chem.* **2019**, *1*, 77–89.
- [10] Z. Lei, F. Zhang, *Angew. Chem. Int. Ed.* **2021**, *60*, 16294–16308.
- [11] J. C. Er, M. K. Tang, C. G. Chia, H. Liew, M. Vendrell, Y.-T. Chang, *Chem. Sci.* **2013**, *4*, 2168–2176.
- [12] Y. Hong, J. W. Y. Lam, B. Z. Tang, *Chem. Soc. Rev.* **2011**, *40*, 5361–5388.
- [13] Y. Yang, X. Su, C. N. Carroll, I. Aprahamian, *Chem. Sci.* **2012**, *3*, 610–613.
- [14] H. Qian, M. E. Cousins, E. H. Horak, A. Wakefield, M. D. Liptak, I. Aprahamian, *Nat. Chem.* **2017**, *9*, 83–87.
- [15] L. A. Tatum, X. Su, I. Aprahamian, *Acc. Chem. Res.* **2014**, *47*, 2141–2149.
- [16] A. N. Bismillah, I. Aprahamian, *J. Phys. Org. Chem.* **2023**, *36*, e4485.
- [17] Y. Yang, R. P. Hughes, I. Aprahamian, *J. Am. Chem. Soc.* **2012**, *134*, 15221–15224.
- [18] Q. Qiu, Q. Qi, J. Usuba, K. Lee, I. Aprahamian, G. G. D. Han, *Chem. Sci.* **2023**, *14*, 11359–11364.
- [19] Y. Yang, R. P. Hughes, I. Aprahamian, *J. Am. Chem. Soc.* **2014**, *136*, 13190–13193.
- [20] D. Cappello, D. A. B. Therien, V. N. Staroverov, F. Lagugné-Labarthe, J. B. Gilroy, *Chem. Eur. J.* **2019**, *25*, 5994–6006.
- [21] D. Cappello, A. E. R. Watson, J. B. Gilroy, *Macromol. Rapid Commun.* **2021**, *42*, 2000553.
- [22] D. Cappello, R. R. Maar, V. N. Staroverov, J. B. Gilroy, *Chem. Eur. J.* **2020**, *26*, 5522–5529.
- [23] D. Cappello, F. L. Buguis, P. D. Boyle, J. B. Gilroy, *ChemPhotoChem* **2022**, *6*, e202200131.
- [24] D. Cappello, F. L. Buguis, J. B. Gilroy, *ACS Omega* **2022**, *7*, 32727–32739.
- [25] V. D. Singh, B. K. Dwivedi, Y. Kumar, D. S. Pandey, *Dyes Pigm.* **2021**, *184*, 108812.
- [26] W. Duan, Q. Liu, Y. Huo, J. Cui, S. Gong, Z. Liu, *Org. Biomol. Chem.* **2018**, *16*, 4977–4984.
- [27] J. Zheng, F. Huang, Y. Li, T. Xu, H. Xu, J. Jia, Q. Ye, J. Gao, *Dyes Pigm.* **2015**, *113*, 502–509.
- [28] X. Yan, P. Zhu, Z. Zhou, H. Yang, H. Lan, S. Xiao, *RSC Adv.* **2019**, *9*, 35872–35877.
- [29] V. D. Singh, B. Kumar Dwivedi, Y. Kumar, D. Shankar Pandey, *New J. Chem.* **2021**, *45*, 1677–1685.
- [30] R. R. Maar, J. B. Gilroy, *Chem. Eur. J.* **2018**, *24*, 12449–12457.
- [31] N. Chen, W. Zhang, S. Chen, Q. Wu, C. Yu, Y. Wei, Y. Xu, E. Hao, L. Jiao, *Org. Lett.* **2017**, *19*, 2026–2029.
- [32] Y. Liu, J. Guo, H. Zhang, Y. Wang, *Angew. Chem. Int. Ed.* **2002**, *41*, 182–184.
- [33] P. Li, H. Chan, S.-L. Lai, M. Ng, M.-Y. Chan, V. W.-W. Yam, *Angew. Chem. Int. Ed.* **2019**, *58*, 9088–9094.
- [34] R. B. Alnoman, S. Rihn, D. C. O'Connor, F. A. Black, B. Costello, P. G. Waddell, W. Clegg, R. D. Peacock, W. Herrebut, J. G. Knight, M. J. Hall, *Chem. Eur. J.* **2016**, *22*, 93–96.
- [35] H. Kim, A. Burghart, M. B. Welch, J. Reibenspies, K. Burgess, *Chem. Commun.* **1999**, 1889–1890.

- [36] B. D. Katzman, R. R. Maar, D. Cappello, M. O. Sattler, P. D. Boyle, V. N. Staroverov, J. B. Gilroy, *Chem. Commun.* **2021**, 57, 9530–9533.
- [37] D. J. van Dijken, P. Kovaříček, S. P. Ihrig, S. Hecht, *J. Am. Chem. Soc.* **2015**, 137, 14982–14991.
- [38] D. A. Leigh, V. Marcos, T. Nalbantoglu, I. J. Vitorica-Yrezabal, F. T. Yasar, X. Zhu, *J. Am. Chem. Soc.* **2017**, 139, 7104–7109.
- [39] S. P. Parambil, F. de Jong, K. Veys, J. Huang, S. P. Veettil, D. Verhaeghe, L. V. Meervelt, D. Escudero, M. V. der Auweraer, W. Dehaen, *Chem. Commun.* **2020**, 56, 5791–5794.
- [40] J.-S. Ni, H. Liu, J. Liu, M. Jiang, Z. Zhao, Y. Chen, R. T. K. Kwok, J. W. Y. Lam, Q. Peng, B. Z. Tang, *Mater. Chem. Front.* **2018**, 2, 1498–1507.
- [41] F. M. F. Santos, J. N. Rosa, N. R. Candeias, C. P. Carvalho, A. I. Matos, A. E. Ventura, H. F. Florindo, L. C. Silva, U. Pischel, P. M. P. Gois, *Chem. Eur. J.* **2016**, 22, 1631–1637.
- [42] C. Yu, E. Hao, X. Fang, Q. Wu, L. Wang, J. Li, L. Xu, L. Jiao, W.-Y. Wong, *J. Mater. Chem. C* **2019**, 7, 3269–3277.
- [43] E. W. Ainscough, A. M. Brodie, W. A. Denny, G. J. Finlay, S. A. Gothe, J. D. Ranford, *J. Inorg. Biochem.* **1999**, 77, 125–133.
- [44] L. Zhang, G.-C. Xu, H.-B. Xu, V. Mereacre, Z.-M. Wang, A. K. Powell, S. Gao, *Dalton Trans.* **2010**, 39, 4856–4868.
- [45] S. Mondal, S. Naskar, A. K. Dey, E. Sinn, C. Eribal, S. R. Herron, S. K. Chattopadhyay, *Inorg. Chim. Acta* **2013**, 398, 98–105.
- [46] Y. Singh, R. N. Patel, S. K. Patel, R. N. Jadeja, A. K. Patel, N. Patel, H. Roy, P. Kumar, R. J. Butcher, J. P. Jasinski, M. Cortijo, S. Herrero, *Polyhedron* **2021**, 200, 115142.
- [47] Deposition numbers 2297990 (for **2a**), 2297991 (for **2d**), and 2297992 (for **2f**) contain the supplementary crystallographic data for this paper. These data are provided free of charge by the joint Cambridge Crystallographic Data Centre and Fachinformationszentrum Karlsruhe Access Structures service.
- [48] O. A. Vydrov, G. E. Scuseria, *J. Chem. Phys.* **2006**, 125, 234109.
- [49] T. M. Henderson, A. F. Izmaylov, G. Scalmani, G. E. Scuseria, *J. Chem. Phys.* **2009**, 131, 044108.
- [50] S. Dong, Z. Li, J. Qin, *J. Phys. Chem. B* **2009**, 113, 434–441.
- [51] S.-Y. Kim, Y.-J. Cho, G. F. Jin, W.-S. Han, H.-J. Son, D. W. Cho, S. O. Kang, *Phys. Chem. Chem. Phys.* **2015**, 17, 15679–15682.
- [52] Z. R. Grabowski, K. Rotkiewicz, W. Rettig, *Chem. Rev.* **2003**, 103, 3899–4032.
- [53] N. J. Hestand, F. C. Spano, *Chem. Rev.* **2018**, 118, 7069–7163.
- [54] J. H. Kim, T. Schembri, D. Bialas, M. Stolte, F. Würthner, *Adv. Mater.* **2022**, 34, 2104678.
- [55] J. Mei, N. L. C. Leung, R. T. K. Kwok, J. W. Y. Lam, B. Z. Tang, *Chem. Rev.* **2015**, 115, 11718–11940.
- [56] K. Yuan Chiu, T. Xiang Su, J. Hong Li, T.-H. Lin, G.-S. Liou, S.-H. Cheng, *J. Electroanal. Chem.* **2005**, 575, 95–101.
- [57] J. F. Ambrose, R. F. Nelson, *J. Electrochem. Soc.* **1968**, 115, 1159.
- [58] M. J. Frisch, G. W. Trucks, H. B. Schlegel, G. E. Scuseria, M. A. Robb, J. R. Cheeseman, G. Scalmani, V. Barone, G. A. Petersson, H. Nakatsuji, X. Li, M. Caricato, A. V. Marenich, J. Bloino, B. G. Janesko, R. Gomperts, B. Mennucci, H. P. Hratchian, J. V. Ortiz, A. F. Izmaylov, J. L. Sonnenberg, D. Williams-Young, F. Ding, F. Lipparini, F. Egidi, J. Goings, B. Peng, A. Petrone, T. Henderson, D. Ranasinghe, V. G. Zakrzewski, J. Gao, N. Rega, G. Zheng, W. Liang, M. Hada, M. Ehara, K. Toyota, R. Fukuda, J. Hasegawa, M. Ishida, T. Nakajima, Y. Honda, O. Kitao, H. Nakai, T. Vreven, K. Throssell, J. A. Montgomery Jr., J. E. Peralta, F. Ogliaro, M. J. Bearpark, J. J. Heyd, E. N. Brothers, K. N. Kudin, V. N. Staroverov, T. A. Keith, R. Kobayashi, J. Normand, K. Raghavachari, A. P. Rendell, J. C. Burant, S. S. Iyengar, J. Tomasi, M. Cossi, J. M. Millam, M. Klene, C. Adamo, R. Cammi, J. W. Ochterski, R. L. Martin, K. Morokuma, O. Farkas, J. B. Foresman, D. J. Fox, *Gaussian 16*, Revision B.01; Gaussian Inc.: Wallingford, CT, **2016**.
- [59] Bruker-AXS, SAINT version 2013.8, **2013**, Bruker-AXS, Madison, WI, USA.
- [60] Bruker-AXS, SADABS, version 2012.1, **2012**, Bruker-AXS, Madison, WI, USA.
- [61] G. M. Sheldrick, *Acta Crystallogr.* **2015**, A71, 3–8.
- [62] G. M. Sheldrick, *Acta Crystallogr.* **2015**, C71, 3–8.
- [63] C. F. Macrae, I. J. Bruno, J. A. Chisholm, P. R. Edgington, P. McCabe, E. Pidcock, L. Rodriguez-Monge, R. Taylor, J. van de Streek, P. A. Wood, *J. Appl. Crystallogr.* **2008**, 41, 466–470.
- [64] M. Kuriakose, M. R. P. Kurup, E. Suresh, *Spectrochim. Acta A. Mol. Biomol. Spectrosc.* **2007**, 66, 353–358.

---

Manuscript received: February 16, 2024  
Revised manuscript received: February 21, 2024  
Accepted manuscript online: February 23, 2024  
Version of record online: March 11, 2024